

INTERNATIONAL SOCIETY FOR SOIL MECHANICS AND GEOTECHNICAL ENGINEERING



This paper was downloaded from the Online Library of the International Society for Soil Mechanics and Geotechnical Engineering (ISSMGE). The library is available here:

<https://www.issmge.org/publications/online-library>

This is an open-access database that archives thousands of papers published under the Auspices of the ISSMGE and maintained by the Innovation and Development Committee of ISSMGE.

The paper was published in the proceedings of the 20th International Conference on Soil Mechanics and Geotechnical Engineering and was edited by Mizanur Rahman and Mark Jaksa. The conference was held from May 1st to May 5th 2022 in Sydney, Australia.

Behavior of soil slope under application of wetting and drying cycles

Comportement de la pente du sol sous l'application des cycles de mouillage et de séchage

Ga Zhang & Fangyue Luo

State Key Laboratory of Hydrosience and Engineering, Tsinghua University, 100084, Beijing, P R China.

ABSTRACT: Soil slopes often undergo wetting and drying cycles in natural circumstances, which is one of the most common causes of slope failures. Thus, centrifuge model tests were conducted to investigate the deformation and failure behavior of soil slopes under wetting and drying cycles. The influence of the wetting and drying cycles were analyzed by comparing the experimental observations and full field displacement measurements. Test results show that a downward progressive failure, namely from the slope top to the slope bottom, occurred on the soil slope during wetting and drying cycles. The progressive failure exhibits significant coupling characteristic between the deformation localization and the local failure. On one hand, the wetting and drying cycles induce deformation localization that gradually develops and eventually causes the local failure at the corresponding location. On the other hand, the local failure remarkably exacerbates the development of the deformation localization. Therefore, the wetting and drying cycles decrease the stability level of the slope by inducing significant shear deformation. The slope deformation is found out to be greatly reduced during the subsequent loading process after the slope went through the wetting and drying cycles. The influential mechanism is that the wetting and drying cycles decrease the void ratio and thus increase the deformation modulus of the soil.

RÉSUMÉ : Les pentes du sol subissent souvent des cycles de mouillage et d'assèchement dans des circonstances naturelles, ce qui est l'une des causes les plus fréquentes de l'effondrement des pentes. Ainsi, des essais sur modèle de centrifugeuse ont été réalisés pour étudier le comportement de déformation et de rupture des pentes du sol lors des cycles de mouillage et de séchage. L'influence des cycles de mouillage et de séchage a été analysée en comparant les observations expérimentales et les mesures de déplacement en plein champ. Les résultats des tests montrent qu'une défaillance progressive vers le bas, c'est-à-dire du haut de la pente vers le bas, s'est produite sur la pente du sol pendant les cycles de mouillage et de séchage. La défaillance progressive présente une caractéristique de couplage significative entre la localisation de la déformation et la défaillance locale. D'une part, les cycles de mouillage et de séchage induisent une localisation de la déformation qui se développe progressivement et finit par provoquer la défaillance locale à l'endroit correspondant. D'autre part, l'échec local exacerbe remarquablement le développement de la localisation de la déformation. Par conséquent, les cycles de mouillage et de séchage diminuent le niveau de stabilité de la pente en induisant une importante déformation par cisaillement. Il s'avère que la déformation de la pente est fortement réduite lors du processus de chargement suivant, après que la pente ait subi les cycles de mouillage et de séchage. Le mécanisme influent est que les cycles de mouillage et de séchage diminuent le taux de vide et augmentent ainsi le module de déformation du sol.

KEYWORDS: Slope, wetting-drying cycle, deformation, failure.

1 INTRODUCTION.

Soil often undergoes wetting and drying cycles in natural and thus causes failure of soil structures. For example, 90% failure of the slopes near the reservoirs were related to the water variation (Vater et al. 2019; Chen et al. 2020). It is of significance to develop an effective analysis method for evaluation of safety level of soil slopes under application of wetting and drying cycles. Some researches focused on the safety analysis targeting on the slope under wetting and drying cycles (Gu et al. 2020; Yuan et al. 2020).

Numerical simulations have been used to investigate the slope response under the condition of wetting and drying (Yu et al. 2019; Wang et al. 2020). Centrifuge model tests are also an effective approach for failure mechanism study on the slopes and have been employed to a wide variation of conditions (Ng et al. 2015; Luo and Zhang 2016; Wang et al. 2017). However, the effect of wetting-drying cycles has not been systematically considered on the slope deformation and failure using centrifuge modeling.

In this paper, centrifuge model tests were conducted to investigate the deformation and failure behavior of slopes under wetting and drying cycles. The influence rules and mechanism of the wetting and drying cycles were analyzed by comparing the experimental observations and full field displacement measurement under different wetting and drying conditions.

2 TEST DESCRIPTION

2.1 Devices

The Tsinghua 50 g-ton geotechnical centrifuge was used for the centrifuge model tests in this paper. The model was placed in the model container with a length of 600 mm, a width of 200 mm and a height of 500 mm (Figure 1). It should be noted that the model container was equipped with an organic glass to observe the model in it.

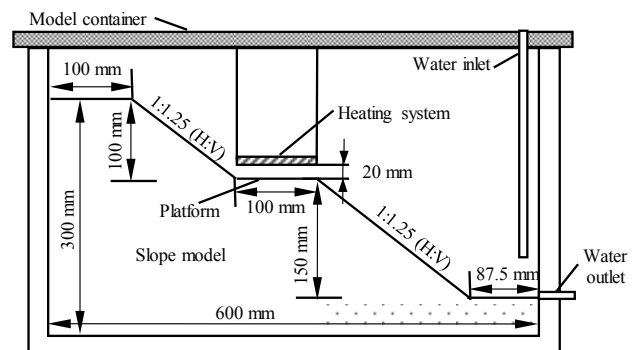


Figure 1. Schematic view of the model (unit: mm).

The wetting and drying cycles were realized by a water variation simulator and heating system in the centrifuge model tests. The wetting was realized by raising the water level with the

water variation simulator (Luo and Zhang 2016). To simulate the drying process, the water level was decreased using the water variation simulator and then the heating system was mobilized to accelerate the drying process (Luo and Zhang 2018).

2.2 Model

The slope model was made of a type of silty clay whose specific gravity is 2.7. The plastic limit and liquid limit of the soil are 15.5% and 33.5%, respectively. The dry density of the soil is 1.6 g/cm³ and the initial water content is 18% for the model preparation.

Figure 1 shows the schematic view of the slope model. The slope model consists of two slope parts with gradient of 1:1.25 (Vertical: Horizontal). The height of the upper slope part is 100 mm and the height of the lower slope part is 150 mm. A 100-mm-long platform was designed between the two parts. The slope top is 100 mm wide. And a 50-mm-thick soil layer is set under the slope bottom to reduce the effect of the model container on the slope during tests.

The slope model was obtained by compacting by layers with a thicknesses of 50 mm and then removing the surplus soil. The side of the slope model with contact to the organic glass was embedded with white particles for significant grey differences according to the requirement of the image-based measurement. The friction between the model container and the slope model was sufficiently reduced by smearing silicone oil.

The heating system was horizontally attached on the model container with a distance of 20 mm from the flatform.

2.3 Test Scheme and procedure

The wetting-drying cycles were simulated in the centrifuge model tests at 50 g level. The changing rate of water level is set to 2.0 mm/s. The test procedures are as follows:

(1) The centrifugal acceleration was increased with sub-increment of 10 g and then reached 50 g. During each loading step was completed, the centrifugal acceleration was maintained about 5 min to permit the self-weight induced deformation of the slope became stable at that g level.

(2) At 50 g level, the water level was increased to 200 mm high from the toe of the slope with four sub-step of 50 mm. During each water increment, the water level was maintained about 10 min to permit the slope deformation stable.

(3) The water level was decreased to 100 mm high from the toe of the slope and then the heating system was turned on to bake the slope for 15 min.

(4) The water level was increased to 200 mm high from the toe of the slope and maintained about 20 min.

(5) The water level was decreased to 100 mm high from the toe of the slope and then the heating system was turned on to bake the slope for 15 min for the second time.

(6) The water level was increased to 200 mm high from the toe of the slope and maintained about 20 min for the second time.

(7) After two wetting and drying cycles, the water level was decreased to the toe of the slope rapidly and the test was ended.

In comparison with the wetting and drying cycle application, the other centrifuge model test was conducted to simulate the direct drawdown conditions. In this test, the above steps (1)-(2) was carried out and then the water level was decreased to the toe of the slope rapidly and the test was ended. The test of wetting and drying cycles is abbreviated as T1, the other test of direct drawdown condition is abbreviated as T2.

2.4 Measurement

During the tests, an image-capture and displacement-measurement system was used to capture the pictures and record the video of the slope and water level change. The water level was determined according to the captured images. In addition,

the correlation-based analysis was employed to determine the displacement history of an arbitrary point on the lateral side of the slope using the captured image series (Zhang et al. 2009). The measurement accuracy of the slope displacement is 0.03 mm.

All the measurement results, including the water level and displacement, are presented in the model scale. According to the similarity law of centrifuge model tests, the prototype dimension could be determined through multiplying the model dimension with the magnitude of the g level, 50.

3 OBSERVATIONS

3.1 Failure behavior

The slope exhibits a remarkable landslide during drawdown after two wetting and drying cycles. Figure 2 shows the photograph after the test and outlines the slip surface. The slip surface was sketched in red dashed line (Figure 3). A Cartesian coordinate is set up to describe the slope response accurately. The origin of the coordinate is set at the toe of the slope and the positive directions of the x-axis and y-axis are rightwards and upwards, respectively (Figure 3).

It can be seen that the landslide appears the lower part of the slope. The slip surface is curved from the flatform to the toe of the slope. On the contrary, the slope does not exhibit failure due to the drawdown if it has not experienced the wetting and drying cycles according to the test observations.

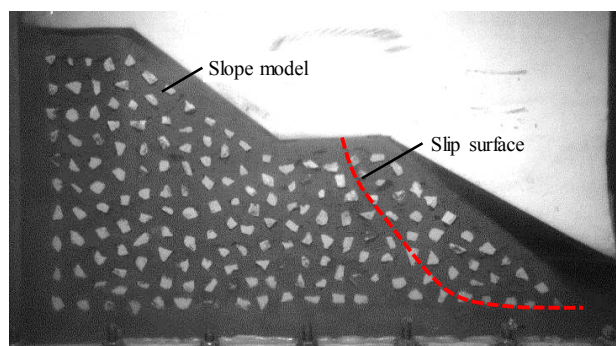


Figure 2. Photograph of the slope after the test with wetting and drying cycles with sketch of the slip surface.

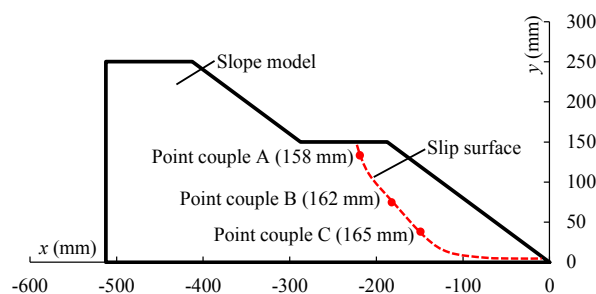


Figure 3. Schematic view of the slip surface of the slope.

Point couple analysis was used to determine the failure process of the slope under wetting and drying cycles. A couple of points are selected on the both sides of the slip surface with a distance of 6 mm. The change of water level of point couples A, B and C at local failure moment are indicated in the brackets (Figure 3). The y coordinates of the point couples A, B and C are 135 mm, 75 mm and 35 mm, respectively. The relative

displacements of the points were determined using the image-based analysis and decomposed to two components that are tangential and normal to the slip surface.

Figure 4 shows the histories of the relative displacement of the point couples A, B and C during final drawdown after wetting and drying cycles. It can be seen that the relative displacement increased as the water level decreases. There is an inflection point on the history curve of the tangential relative displacement, after which the relative displacement increases rapidly. It can be inferred that the local failure occurs at the inflection point. Thus, the inflection point could be regarded as the local failure moment of the slope, which are outlined using the dashed lines in Figure 4. This result indicates that the slip surface developed from the flatom to the toe of the slope. In other words, the drawdown induces a downward progressive failure of the slope, which is similar to the previous observations (Luo and Zhang 2016).

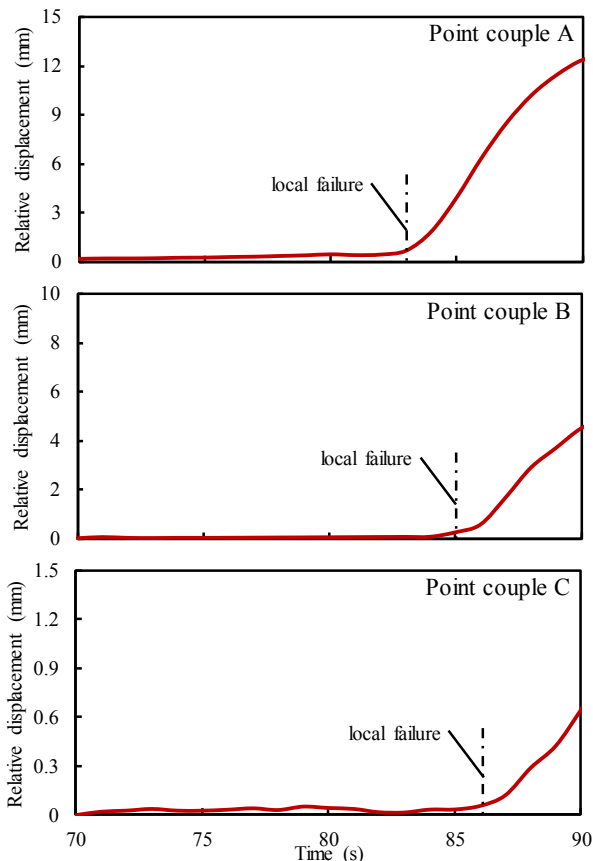
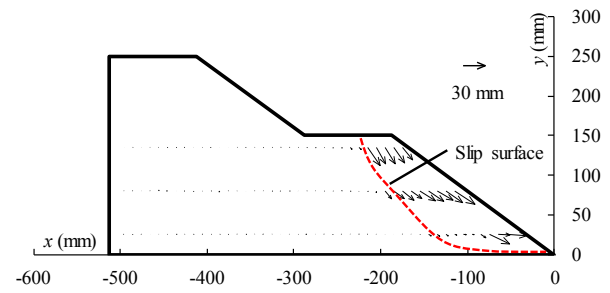
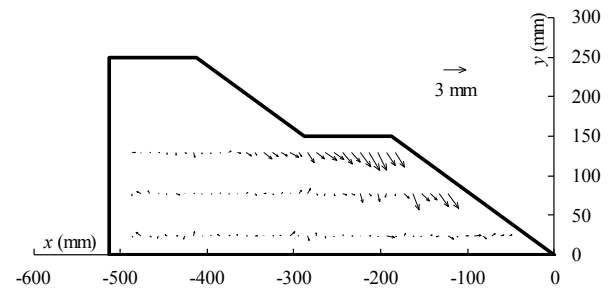


Figure 4. Histories of the tangential relative displacement of the point couples during final drawdown after wetting and drying cycles.

Figure 5 compares the vector of displacement of the slopes after tests where the wetting and drying cycles are carried out or not. It can be seen from Figure 5 that the wetting and drying cycles significantly affect the displacement distribution of the slope. For the slope experiencing the wetting and drying cycles, the drawdown induced displacement concentrates in the lower part of the slope and near the slope surface, where a landslide occurs. On the other hand, the slope that has not experienced the wetting and drying cycles, the drawdown induced displacement concentrates in the upper part of the slope and near the top of the slope. It can be concluded that the wetting and drying cycles decrease the stability level of the slope and changes the displacement distribution under drawdown conditions.



(a) Drawdown after wetting and drying cycles



(b) Drawdown directly

Figure 5. Displacement vectors of the slope with schetch of the slip surface. (time: 90 s in final drawdown).

3.2 Deformation behavior

The effect of the wetting and drying cycles on the deformation could be further analyzed on the basis of displacement observations. Figure 6 shows the settlement histories of typical point M on the slope during final drawdown under different test conditions. It can be seen that the settlement increases as the water level decreases for both the tests. The final drawdown induced settlement was decreased by the prior wetting and drying cycles, whether on the upper and lower parts of the slope.

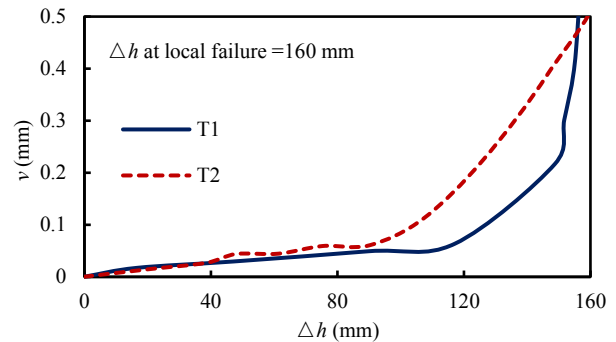


Figure 6. Histories of displacement of typical point M ($x = -195$ mm, $y = 125$ mm) on the slope during drawdown under different test conditions. v , vertical displacement; Δh , change of water level.

Figure 7 compares the distribution of settlement of the slopes induced by the final drawdown under different test conditons. It can be found that the final drawdown induced settlement increased from the interior to the surface of the slope at an elevation. Such the settlement becomes smaller if the slope experiences wetting and drying cycles. This result indicates that the wetting and drying cycles causes a smaller deformation induced by the final drawdown.

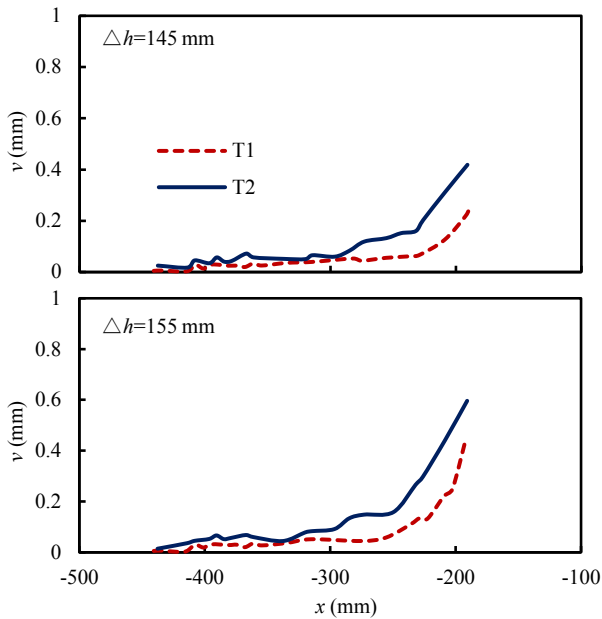


Figure 7. Horizontal distributions of final drawdown induced settlement of the slopes under different conditions ($y=125$ mm). v , vertical displacement; Δh , change of water level

The wetting and drying cycle induced settlement is outlined for different cycles (Figure 8). It can be seen that first wetting and drying cycle induces a larger settlement than the second wetting and drying cycle. This result indicates that the wetting and drying cycle induced deformation of the slope decreases with increasing number of wetting and drying cycles.

In summary, it can be concluded that the wetting and drying cycles have a significant effect on reducing the deformation induced the subsequent loading. In other words, the wetting and drying cycles increase the stiffness of the slope.

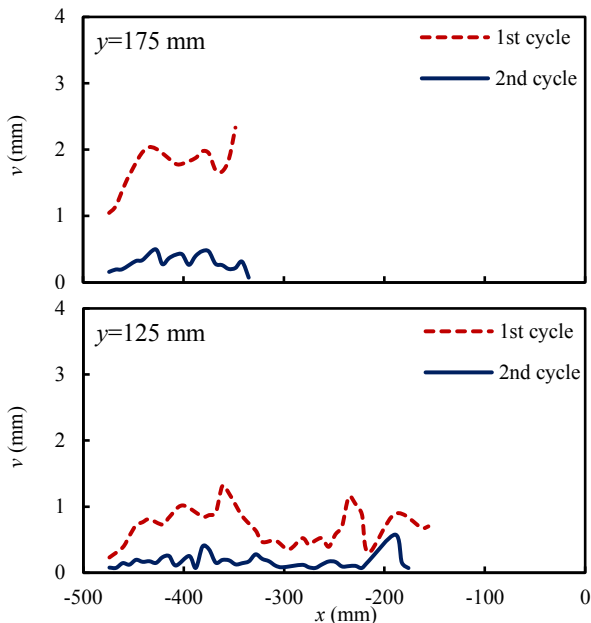


Figure 8. Horizontal distributions of wetting and drying cycle induced settlement of the slopes. v , vertical displacement.

4 MECHANISM ANALYSIS

The failure mechanism of the slope was analyzed using the integrated scheme of deformation and failure processes (Zhang

and Wang 2016). Figure 9 shows the horizontal distribution of maximum shear strain of the slope due to the final drawdown. In the figure, the corresponding local failure moment and location are indicated. It can be seen that the shear strain is fairly small as the water level decreases in the first period. The shear strain becomes more prominent and concentrates in a narrow zone (Figure 9 (a)). This demonstrates that there is a deformation localization that intensifies as the water level decreases. The local failure then appears in the localization area. It can be inferred that the deformation localization develops and cause the local failure there. It can be seen from Figure 9 (b) that the shear strain increases significantly after local failure with decreasing water level. This result demonstrates that the local failure causes new deformation localization. It can be found in Figure 9 that the shear strain distribution curves within the localization area are similar for different water levels. Thus, the maximum shear strain at the slip surface could be used as an index to the extent of localization.

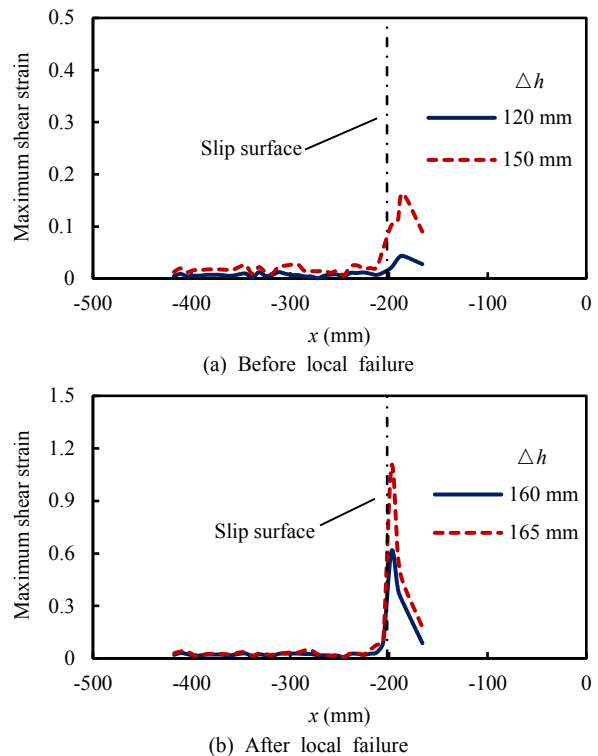


Figure 9. Horizontal distributions of maximum shear strain of the slope ($y=125$ mm, Δh at local failure =160 mm). Δh , change of water level.

Figure 10 shows the histories of maximum shear strain at the slip surface of the slope during wetting and drying cycles. It can be seen that the shear strain increases during the wetting and drying cycles. This result indicates that the wetting and drying cycles induce localization continuously. Such localization accumulation contributes the slope failure during final drawdown. For the directly drawdown condition, there is not the localization accumulation and avoid slope failure during the final drawdown.

Figure 11 shows the maximum shear strains of typical points on the slope during final drawdown under different test conditions. It can be seen that the shear strain increases as the water level decreases for both the tests. It can be inferred that the wetting and drying cycles induce shear deformation in the slope that causes the deformation localization in the slope.

Figure 12 shows the histories of void ratio change on the slope during wetting and drying cycles. It can be seen that the void ratio decreases during wetting and drying cycles. Compared the initial

void ratio, the void ratio after wetting and drying cycles becomes small. This result indicates that the wetting and drying cycles cause the slope become more denser and thus increase the deformation modulus of the soil before the final drawdown. This result leads to the fact that the final drawdown induced deformation became small if the slope experiences the wetting and drying cycles.

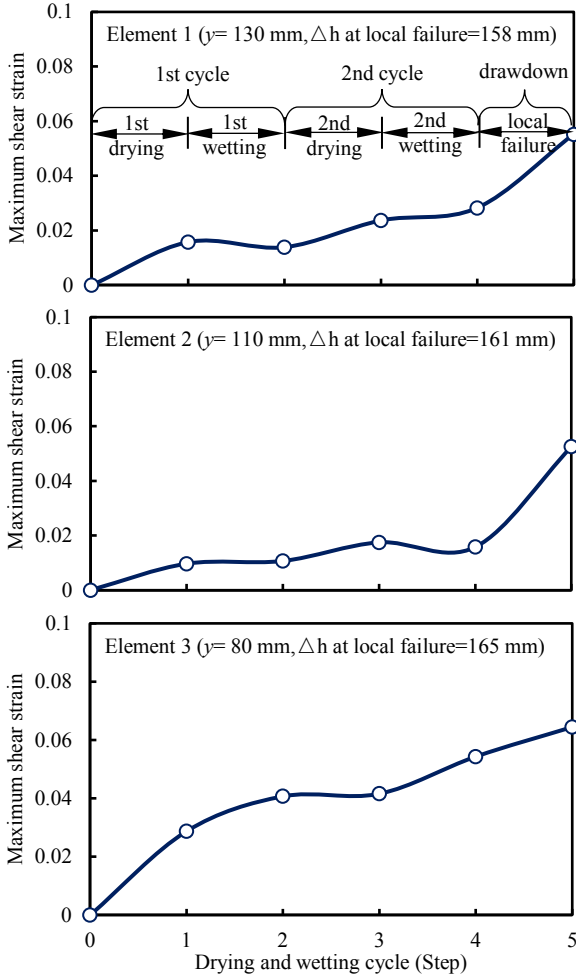


Figure 10. Histories of maximum shear strain at the slip surface of the slope.

5 CONCLUSIONS

Centrifuge model tests were performed to investigate the effect of the wetting and drying cycles on the behavior of the slopes. According to the comparisons of the test observations, the following conclusions were obtained:

- The slope exhibits a downward progressive failure during wetting and drying cycles.
- The wetting and drying cycles induce deformation localization that develops and causes the local failure there. The local failure causes new deformation localization.
- The wetting and drying cycles decrease the stability level of the slope. The reason is that the wetting and drying cycles induce shear deformation that causes the deformation localization in the slope.
- The wetting and drying cycles reduces the deformation induced the subsequent loading. The influential mechanism

is that the wetting and drying cycles decrease the void ratio and thus increase the deformation modulus of the soil.

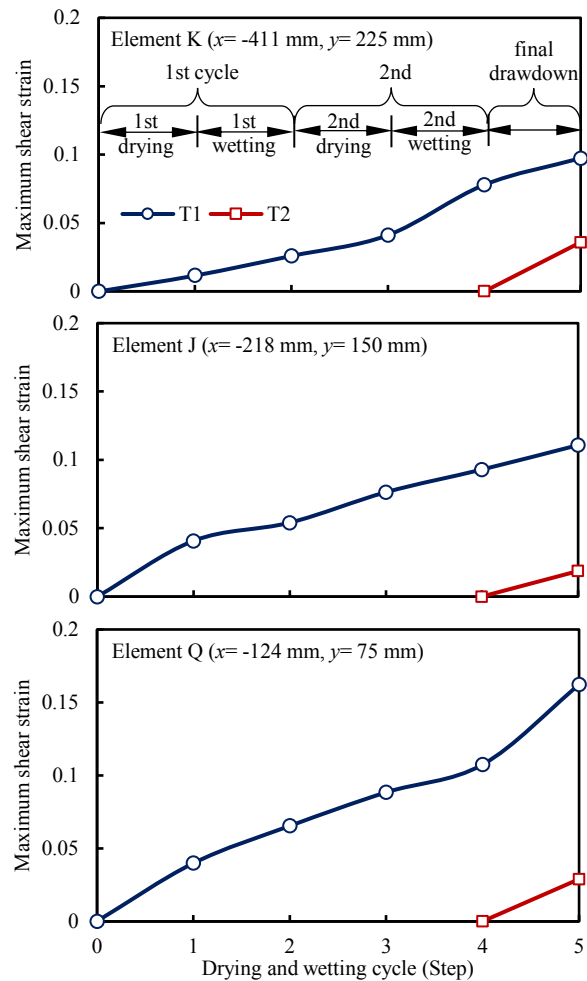


Figure 11. Histories of maximum shear strains on the slope during drawdown under different test conditions.

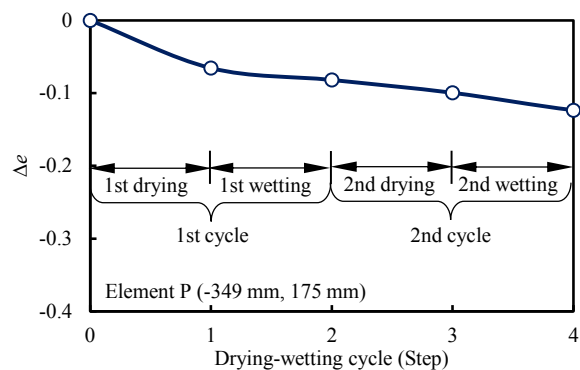


Figure 12. Histories of void ratio change on the slope during wetting and drying cycles. Δe , change of void ratio.

6 ACKNOWLEDGEMENTS

The study is supported by the National Natural Science Foundation of China under Grant (52039005) and Open Research Fund Program of State key Laboratory of Hydrosience and Engineering (sklhse-2020-D-03).

7 REFERENCES

- Chen, Y.L., Withanage, K.R., Uchimura, T., Mao, W.W., Nie, W. 2020. Shear deformation and failure of unsaturated sandy soils in surface layers of slopes during rainwater infiltration. *Measurement*, 149.
- Gu, X., Wang, L., Chen, F.Y., Li, H.R., Zhang, W.G. 2020. Reliability analysis of slope stability considering temporal variations of rock mass properties. *Computers Materials & Continua*, 63(1): 263-281.
- Luo, F.Y., Zhang, G. 2016. Progressive failure behavior of cohesive soil slopes under water drawdown conditions. *Environmental Earth Sciences*, 75(11): 973
- Luo, F.Y., Zhang, G. 2018. Centrifuge model test on deformation and failure of slopes under wetting-drying cycles. *9th International Conference on Physical Modelling in Geotechnics*, London UK: 1137-1142
- Ng, C.W.W., Kamchoom, V., Leung, A.K. 2015. Centrifuge modelling of the effects of root geometry on transpiration-induced suction and stability of vegetated slopes. *Landslides*, 3(5): 925-938
- Vater, S., Beisiegel, N., Behrens, J. 2019. A limiter-based well-balanced discontinuous Galerkin method for shallow-water flows with wetting and drying: Triangular grids. *International Journal For Numerical Methods In Fluids*, 91(8):395-418
- Wang, J.M., Chapman, D., Yang, X.J. 2020. Investigating the stability and anchor support parameters of slopes subjected to wetting and drying cycles in relation to the Nanfen open-pit mine, China. *Arabian Journal of Geosciences*, 13(20). Doi: 10.1007/s12517-020-06060-9.
- Wang, Y.L., Zhang, G., Wang, A.X. 2017. Progressive failure behavior and mechanism of soil slopes under dynamic loading conditions. *International Journal of Geomechanics*, 17(4): 04016102.
- Yu J.J., Chen D.X., Wang H., Zhang B. 2019. Analysis of the shear strength of granite residual soil and slope stability under wetting-drying cycles. *Journal of Xiamen University (Natural Science)*, 58(4):154-60.
- Yuan S., Si X.D., Zhang S.H. 2020. Shakedown analysis of unsaturated soils considering the variation of hydraulic states. *International Journal of Geomechanics*, 20(9). Doi: 10.1061/(ASCE)GM.1943-5622.0001760.
- Zhang, G., Hu, Y., Zhang, J.M. 2009. New image analysis-based displacement-measurement system for geotechnical centrifuge modeling tests. *Measurement*, 42 (1): 87-96
- Zhang, G., Wang, L. P. 2016. Integrated analysis of a coupled mechanism for the failure processes of pile-reinforced slopes. *Acta Geotechnica*, 11(4): 941-952